Relationship Between Water-soluble Ions and Lidar Depolarization Ratio for Aerosol within the Boundary Layer at Taipei, Taiwan at the Spring of 2004 and 2005

S. Y. Chang[(1)], W. N. Chen[(1)], Charles C. K. Chou[(1)], J. P. Chen[(2)], T. K. Chen[(1)]

[(1)] *Research Center for Environmental Changes, Academia Sinica, Taiwan, wnchen@rcec.sinica.edu.tw*
[(2)] *Atmospheric Science Department, National Taiwan University, Taiwan, jpchen@as.ntu.edu.tw*

ABSTRACT

The optical properties and water-soluble ion of aerosol in boundary layer were measured by lidar and in-situ IC at the spring of 2004 and 2005. Lidar depolarization ratios were compared with mixing ratio of water-soluble ions calcium, potassium, and sodium sampled by ground surface measurements to study the relationship between depolarization and aerosol compositions. About 70% of the daily maximum depolarization ratios for aerosol below boundary layer were distributed between 1.5% and 3.5% with mean value of 2.14±0.83%. High correlation coefficients with R>0.8 were found between depolarization and ion calcium for all of the depolarization episodes (DP≈5%~12%), which suggest the existence of mineral dust. The mixing ratio of K^+ and Na^+ usually are greater than Ca^{2+} but did not show clear dependences with depolarization showing biomass burning and sea salt aerosols may transport along with Asian dust but did not exhibit remarkable non-spherical properties.

1. INTRODUCTION

The particle depolarization is expected to relate with the particle shape [1-3]. A routinely operated depolarization lidar found while Taiwan was suffering under winter monsoon, the depolarization ratio for aerosol below boundary layer may rise from background value (about 2%) to exceed 10% after passage of cold front. Analysis of observational data and model simulation [4] had shown the dust incursion events over Taiwan usually occurred after the passage of a cold front, which was pushed forward by the ocean-bound cutoff high.

Aerosol depolarization ratio is useful for identifying dust aerosols because it indicates non-sphericity of the particle [5]. For spherical particles, depolarization is close to zero. For non-spherical particles, the depolarization ratio of air molecular, dry aerosol may vary from 1.4~2%. Asian dust and biomass burning as reported vary 10~30% [2, 6-7]. Murayama et al. [2] has demonstrated the application of depolarization lidar observations combined with ground measurements to investigate the characteristic of aerosol particles in the boundary layer. Since dust, biomass burning and sea salt are possible source of non-spherical particle. Therefore, to study the relationship between lidar observed high depolarization ratio and Asian dust. Water-soluble ions Ca^{2+}, K^+, and Na^+ are selected as the indicators of mineral dust, biomass burning and sea salt aerosol respectively. [8-9]. The results show high depolarization ratios should be caused by Asian dust, and biomass burning and sea salt aerosols would transport along with Asian dust but did not exhibit remarkable non-spherical properties.

2. METHODS AND EXPERIMENTS

The lidar and aerosol sampling site are located at the weather observatory of the National Taiwan University (25°00'N, 121°32'E), which is located in the southwestern part of the Taipei Basin. During the Asian winter monsoon, the average prevailing wind direction in the Taipei Basin swings between the northeast and the east.

2.1 Lidar

RCEC/ASNTU Lidar is a dual-wavelength Raman and Depolarization Lidar system (manufactured by Zenon SA, Greece). The lidar system employs the second and third harmonics of Nd-YAG laser at 532 nm and 355 nm. More details are provided in Table 1. This system is 24 hours operated to probe the atmosphere in the height range between 0.3 km and 8 km.

Aerosol backscattering ratio R is define as:

$$R_\lambda(z) = 1 + \frac{\beta_a(\lambda, z)}{\beta_m(\lambda, z)} \quad (1)$$

For nighttime measurement, the calculation of β_a (or R) is basing on Raman inversion algorithm by Ansmann *et al.* [10]. For daytime measurement, the calculation of aerosol backscatter is using the Klett's method [11] with a range-depended lidar ratio obtained from nighttime Raman measurements. The depolarization ratio is defined as the ratio of the return light of perpendicular to parallel polarizations, as given by the following equation:

$$DP = P_\perp / P_\parallel \quad (2)$$

where $P_{\perp}$ and $P_{\parallel}$ are the integrated return power for parallel and perpendicular directions relative to the outgoing laser beam.

Table 1. Lidar Characteristics

Laser	Nd:YAG (Big-Sky CFR-400)
Wavelength	532/355 nm
Pulse energy	65/60 mJ
Repetition rate	20 Hz
Transient Record	12 bits A/D converter at 20 MHz and 250 MHz photon counting (Licel TR20-40)
Height Resolution	7.5 m
Telescope	diameter 40 cm, focal length 160 cm
Channels	532 (*S* and *P*), 355 nm, and 387 nm (nighttime only)

2.2 In-situ IC

The aerosol composition was analysis by an in-situ IC system, which provides concentration of water-soluble ions Cl^-, NO_2^-, NO_3^-, SO_4^{2-}, Na^+, NH_4^+, K^+, and Ca^{2+}. The in-situ IC system consisted of the following: gas removal denuders, aerosol collecting device and ion chromatograph (Model ICS-90, Dionex Corp., Sunnyvale, CA, YSA). The in-situ IC system is attached to the bypass flow line of the TEOM monitor, to semi-continuously measure the water-soluble inorganic ions of PM10 (at spring of 2004) or PM2.5 (at spring of 2005) at intervals of 15-min.

3. RESULTS AND DISCUSSIONS

During the sampling period (2004 spring and 2005 spring), there are 124 lidar operation days available for depolarization calculation. The occurrence frequency of daily maximum depolarization ratio (hourly averaged) below boundary layer is shown in Fig. 1. The typical backscattering ratio for aerosol inside boundary layer is R≈10±5, therefore, depolarization ratio is close to particle depolarization. As shown in Fig. 1, about 70% of the daily maximum total depolarization ratios for aerosol below boundary layer is distributed between 1.5% and 3.5%, which is much close to reported particle depolarization ratio of generic aerosols [12].

When Taiwan was suffered by winter monsoon, the total depolarization ratio for aerosol below boundary layer was usually found to rise from background value to exceed 10%. The duration of each depolarization episode varies from few hours to more than 3 days and the height may up to 1.5 km. The maximum depolarization of such cases varies from about 5% to 12%. During the depolarization episodes, surface ground aerosol measurements (PM_{10} and $PM_{2.5}$) also found the mass ratio of coarse mode to fine mode particles tend to increase with increasing of depolarization. To investigate the reason cause the rising of aerosol depolarization, water-soluble ions of aerosol were selected to study the correlation between depolarization and aerosol compositions. The mean depolarization ratios for all non-dust days and Asian dust episodes are 2.14±0.83% and 6.22±1.48% respectively. The observed depolarization ratios are close to dust measured at China, Japan, and Korea.

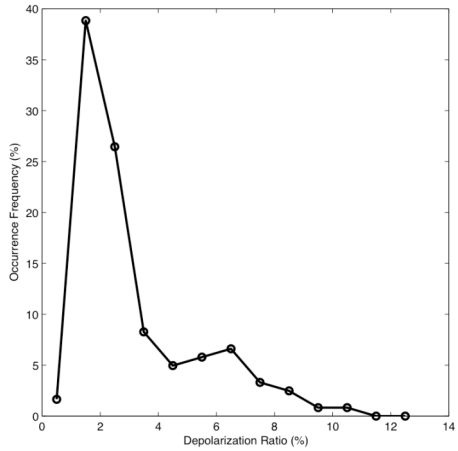

Fig. 1. Occurrence frequencies of depolarization ratio DP observed at height below boundary layer during the sampling period.

A typical depolarization episode occurred during 2/14 ~ 2/17, 2004 observed lidar is shown in Fig. 2. During 2/14 18:00L to 2/15 12:00L, an aerosol layer with higher backscattering ratio about R_{355}≈9 (R_{532}≈20, not shown) were found right after arrive of a front (figure 3c). Aerosol depolarization ratio was found starting to rise at 2/15 0:00L and maintaining at a higher depolarization ratio about *DP* ≈ 3.5~6% between 2/15 9:00L and 2/17 22:00L implying the existence of non-spherical particles. The backscattering ratio is about R_{532}≈10 (R_{355}≈3) for this depolarization layer. Vertical distribution of backscattering ratio indicates non-spherical particles meanly located below boundary layer at height below about 1000 m during this depolarization episode.

A layer with high backscattering ratio about R_{532}≥150 located at height 1.2~1.7 km could be found at morning of 2/15. Radiosonde data shows the relative humidity at that height range is RH≥90% (Figure 3c), indicating this layer should be a cloud and the high depolarization (DP ≈ 5%) may be caused multi-scattering effect.

In order to study the relationship between particle depolarization and aerosol compositions, water-soluble ions Ca^{2+}, K^+, and Na^+ selected to compare with depolarization as shown in Fig. 2e. Fig. 2e shows temporal evolution of total depolarization ratio and

mass fraction of ions Ca (Ca^{2+}/PM_{10}), K (K^{+}/PM_{10}), and Na (Na^{+}/PM_{10}) during 2004/2/14 12:00L ~ 2/17 24:00L. Obviously, only Ca^{2+}/PM_{10} exhibit same tendency as DP. The correlation coefficient between *DP* and ions Ca, K, and Na are 0.824, -0.147, and 0.461 respectively. Because the observed value of DP reflects contributions from all kinds of aerosols, so the higher value of DP implies that the percentage of nonspherical particles is higher. Since water-soluble Ca^{2+} could be used as tracer of mineral or Asian dust, the high correlation between DP and water-soluble ion Ca strongly recommends that the variation of aerosol depolarization is related with mineral or Asian dust.

Fig. 3 shows another depolarization episode occurred during 4/5 ~ 4/6, 2004. Between 4/5 18:00L to 4/6 18:00L, an aerosol layer with depolarization ratio about 10% was located mainly at height between 0.7~2.3 km. The backscattering ratio is about $R_{532}\approx4$. At 4/6 9:00L~15:00L, vertical distribution of depolarization ratio shows non-spherical particles downward extended from depolarization layer to surface ground, which might be caused by the elevating of internal boundary layer (mixing layer). The comparison between aerosol water-soluble Ca^{2+}, K^{+}, and Na^{+} and depolarization were shown in Fig. 3e. Similar to previous case, only Ca^{2+}/PM_{10} exhibit same temporal variation as DP. And the correlation coefficient is 0.937, which indicated the non-spherical property is contributed by mineral dust.

The correlations between DP and aerosol water-soluble ions for all of the depolarization episodes which both lidar and In-site IC measurements are available are summarized in Table 2. As shown in Table 2, depolarization ratios were found highly correlated with Ca^{2+}/PM_{10} or $Ca^{2+}/PM_{2.5}$ for all of the depolarization episodes, which strongly suggest the observed non-spherical particles were mineral dust. Meteorology and back trajectory analysis show the observed high depolarization episode are outflow of Asian dusts.
As the indicator of biomass burning and sea salt aerosols, the mass fraction of K^{+} and Na^{+} usually are greater than Ca^{2+} but did not show clear dependences with depolarization. Biomass burning and sea salt aerosol mainly exist at find mode particles, $K^{+}/PM_{2.5}$ and $Na^{+}/PM_{2.5}$ for depolarization episodes is about 2 times than that for low-depolarization days. The results show biomass burning and sea salt aerosols may transport along with Asian dust but did not apparently exhibit non-spherical properties.

REFERENCES

1. Sassen, K., The polarization lidar technique for cloud research: A review and current assessment, *Bull. of The Amer. Meteor. Soc.*, Vol. 72, 1848-1866, 1991.

2. Murayama, T., *et al.*, Application of lidar depolarization measurement in the atmospheric boundary layer: Effects of dust and sea-salt particles, *J. Geophy. Res.*, Vol. 104, 31781-31792, 1999.

3. Noel, V., *et al.*, Classification of particle effective shape ratios in cirrus clouds based on the lidar depolarization ratio, *Appl. Opt.*, Vol 41, 4245-4257, 2002.

4. Chen J. P., *et al.*, Simulations of Asian yellow dust incursion over taiwan for the spring of 2002 and 2003, *Terrestrial, Atmospheric and Oceanic Sciences*, Vol. 15, 949-981, 2004.

5. Murayama, T. *et al.*, Ground-based network observation of Asian dust events of April 1998 in east Asia, *J. Geophys. Res.*, Vol. 106, 18,345- 18,359, 2001.

6. Kwon S.A., Iwasaka Y. and Shibata T., Depolarization ratio of air molecules in the free troposphere Lidar measurement in spring 1994, *J. Geomag. Geoelectr.*, Vol 48, 415-419, 1996.

7. Cairo, F., G. D. Donfrancesco, A. Adriani, L. Pulvirenti, and F. Fierli, Comparison of Various linear depolarization parameters measured by lidar, *Appl. Optics*, Vol. 38, 4425-4432, 1999.

8. Mori, I. Y. Iwasaka, K. Matsunaga, M. Hayashi, M. Nishikawa, Chemical characteristics of free tropospheric aerosols over Japan Sea coast: air-borne measurements, *Atmos. Environ.*, Vol. 33, 601-609, 1999.

9. Ma, Y. *et al.*, Characters and influence of biosmoke on the fine-particle ionic composition measured in Asian outflow during Transport and Chemical Evolution Over the pacific (TRACE-P) experiment, *J. Geophys. Res.*, Vol. 108, doi:10.1029/ 2002JD003128, 2003.

10. Ansmann, A., U., *et al.*, Independent measurement of extinction and backscatter profile in cirrus clouds by using a combined Raman elastic-backscatter lidar, *Appl. Opt.*, Vol. 31, 7113-7131, 1992.

11. Klett, J.D., Stable analytic inversion solution for processing lidar returns, *Appl. Opt.*, Vol. 20, 211-220, 1981.

12. Copper, D. W., J. W. Davis, and R. L. Byers, Measurements of depolarization by dry and humidified salt aerosols using a lidar analogue, *Aerosol Science*, Vol 5, 117-123, 1974.

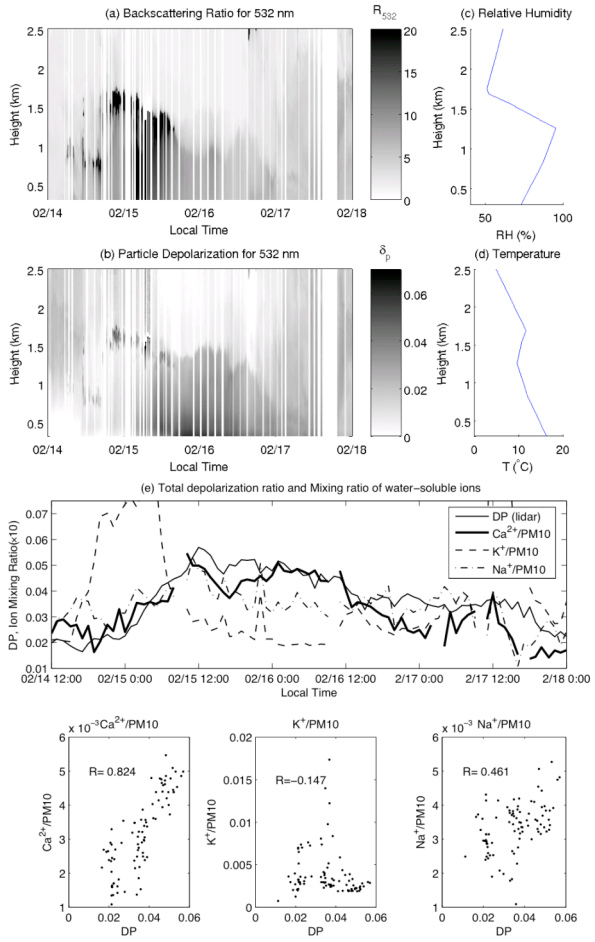

Fig. 2. Lidar observed (a) backscattering and (b) depolarization ratio during 2004/2/14 ~ 2/17. Vertical profile of (c) relative humidity and (d) temperature measured by radiosonde. Time series of (e) depolarization ratio (at 300 m) and mass fraction of ions Ca^{2+}, K^{+}, and Na^{+}.

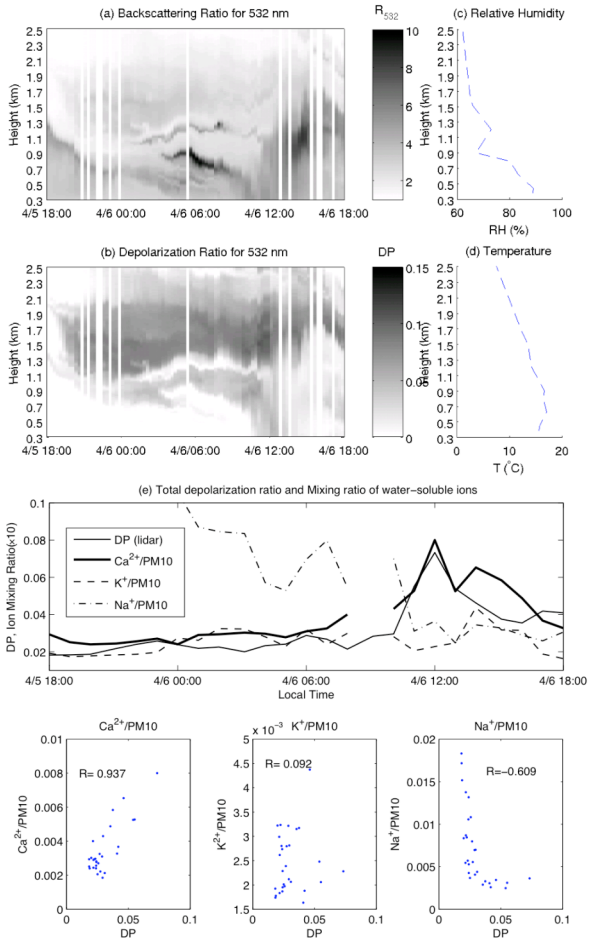

Fig. 3. Same as Fig. 2 but for depolarization episode during 2004/4/5 18:00L~ 4/6 18:00L.

Table 2. The correlation coefficients between depolarization ratio and mass fractions of water-soluble ions ($Ca2^{+}$, K^{+}, Na^{+}).

Depolarization Events	Maximum DP (at 300 m)	Correlation coefficient between DP and mass fraction of ions			Mean mass fraction of ions		
		Ca^{2+}	K^{+}	Na^{+}	Ca^{2+}/PM10	K^{+}/PM10	Na^{+}/PM10
02/14 – 02/17, 2004	7%	0.824	-0.147	0.000	4.07×10^{-3}	4.35×10^{-3}	4.00×10^{-3}
03/15 – 03/16, 2004	5%	0.783	-0.323	0.100	3.21×10^{-3}	1.54×10^{-3}	3.45×10^{-3}
04/02 – 04/03, 2004	12%	0.808	0.285	0.074	13.70×10^{-3}	4.15×10^{-3}	4.84×10^{-3}
04/06, 2004	6%	0.937	0.092	-0.609	4.15×10^{-3}	2.82×10^{-3}	4.70×10^{-3}
Cases above					6.28×10^{-3}	3.21×10^{-3}	4.25×10^{-3}
Cases that DP < 3.5%		-	-	-	2.19×10^{-3}	4.66×10^{-3}	3.15×10^{-3}
		Ca^{2+}	K^{+}	Na^{+}	Ca^{2+}/PM2.5	K^{+}/PM2.5	Na^{+}/PM2.5
03/18 – 03/19, 2005	8%	0.897	0.602	-0.641	8.14×10^{-3}	1.91×10^{-2}	2.67×10^{-2}
03/25, 2005	5%	0.681	0.425	0.352	6.52×10^{-3}	1.19×10^{-2}	5.22×10^{-2}
04/05, 2005	8%	0.752	0.348	-0.421	3.17×10^{-3}	9.61×10^{-3}	1.73×10^{-2}
04/13 - 04/17, 2005	11%	0.777	0.564	-0.823	3.96×10^{-3}	1.94×10^{-2}	4.19×10^{-3}
04/20 - 04/21, 2005	9%	0.724	0.275	0.812	2.95×10^{-3}	1.73×10^{-2}	6.30×10^{-3}
Cases above					4.89×10^{-3}	15.46×10^{-3}	2.14×10^{-2}
Cases DP < 3.5%		-	-	-	1.69×10^{-3}	8.43×10^{-3}	1.03×10^{-2}